

International Journal of Modern Physics E
© World Scientific Publishing Company

Measurement of the multi-hadron decays of ω , K_S^0 and η -mesons in heavy ion collisions at $\sqrt{s_{NN}} = 200$ GeV in the PHENIX experiment at RHIC

V.Ryabov (for the PHENIX Collaboration)

*Petersburg Nuclear Physics Institute, 188300, Russia, Gatchina
riabovvg@mail.pnpi.spb.ru*

Received (received date)

Revised (revised date)

The PHENIX experiment at RHIC measured ω , η and K_S^0 -meson production at high p_T in $p + p$, $d + Au$ and $Au + Au$ collisions at $\sqrt{s_{NN}} = 200$ GeV. Measurements performed in different hadronic decay channels give consistent results. The measured ratios of all three mesons to π^0 are found to be flat as a function of p_T in $p + p$ collisions and equal to $\omega/\pi^0 = 0.81 \pm 0.02 \pm 0.07$, $\eta/\pi^0 = 0.48 \pm 0.02 \pm 0.02$ and $K_S^0/\pi^0 = 0.45 \pm 0.01 \pm 0.05$. Nuclear modification factor measured for ω -mesons in central Au+Au collisions is $R_{AA} = 0.4 \pm 0.15$.

1. Introduction

Hadron spectra measured at high transverse momentum ($p_T > 2$ GeV/c) provide important information on particle production mechanism and properties of the matter produced in RHIC collisions. High- p_T hadrons are mainly produced by fragmentation of partons originating from hard scattering processes. In nucleon-nucleon collisions such processes are relatively well understood and corresponding cross sections can be calculated in perturbative QCD. In nucleus-nucleus collisions various nuclear effects like multiple scattering in the initial state, modification of the parton distribution and fragmentation functions, energy loss in the medium can modify particle production. These effects can be studied by comparison of particle properties measured in $p + p$ and nucleus-nucleus collisions at the same energy. Measurement of ω , η and K_S^0 -meson production in $p + p$, $d + Au$ and $Au + Au$ collisions is a part of systematic study of particle properties at RHIC.

2. Experimental setup and data samples

Two central spectrometers of the PHENIX ¹ experiment ($\Delta\phi < 90^\circ$, $|\eta| < 0.35$) are used to measure neutral and charged particles produced in heavy ion collisions at RHIC. Beam-Beam Counters and Zero Degree Calorimeters provide the minimum bias (MB) trigger, determine z -coordinate of the collision vertex and the

event centrality. Drift Chamber and the first layer of the Pad Chamber are used for reconstruction of charged particle momentum with resolution of $\sigma(p_T)/p_T \approx 1.0\%p_T \oplus 1.1\%$. Two other layers of the Pad Chamber can be used for track confirmation by matching it to the reconstructed hit. High segmentation electromagnetic calorimeter (EMCal) with energy resolution of $\sigma(E)/E \approx 8.1\%/\sqrt{E} \oplus 2.1\%$ is used as a primary detector for reconstruction of γ -quanta and π^0 -mesons ².

The experimental data samples gathered by PHENIX in years 2003-2005 and decays analyzed in these samples are summarized in Table 1. Besides the MB trigger we use high- p_T γ -trigger (γ) realized by adding together amplitudes in 4×4 adjacent EMCal towers and comparing them to a threshold of 1.4 GeV in $p + p$ and 2.4 GeV in $d + Au$ collisions. Only events with the vertex $|z_{vert}| < 30 \text{ cm}$ from the center of the PHENIX experimental region and satisfying various quality assurance cuts are accepted in the analysis.

Table 1. Analyzed decays and data samples.

Run	System	Trig.	Events	$\int L$	Decays	BR (%)	$p_T \text{ (GeV/c)}$
Run3	$p + p$	γ	4.6×10^7	0.22 pb^{-1}	$\eta \rightarrow \pi^0 \pi^+ \pi^-$	22.7 ± 0.4	3 – 8
					$\omega \rightarrow \pi^0 \pi^+ \pi^-$	89.1 ± 0.7	2.75 – 9.25
					$\omega \rightarrow \pi^0 \gamma$	$8.9^{+0.27}_{-0.23}$	2.5 – 6.5
					$K_S^0 \rightarrow \pi^0 \pi^0$	30.7 ± 0.1	2.5 – 6.5
Run3	$d + Au$	γ	2.1×10^7	1.5 nb^{-1}	$\eta \rightarrow \pi^0 \pi^+ \pi^-$		5 – 8
					$\omega \rightarrow \pi^0 \pi^+ \pi^-$		3.5 – 9
					$\omega \rightarrow \pi^0 \gamma$		3 – 7
					$K_S^0 \rightarrow \pi^0 \pi^0$		3.5 – 8.5
Run4	$Au + Au$	MB	7.8×10^8	$129 \text{ } \mu\text{b}^{-1}$	$\omega \rightarrow \pi^0 \gamma$		4 – 9
Run5	$p + p$	MB	1.5×10^9	0.07 pb^{-1}	$\omega \rightarrow \pi^0 \pi^+ \pi^-$		2.25 – 13
		γ	1.0×10^9	2.5 pb^{-1}	$\omega \rightarrow \pi^0 \gamma$		2.5 – 11
					$K_S^0 \rightarrow \pi^0 \pi^0$		2.25 – 10

3. Analysis

As the first step we reconstruct $\pi^0 \rightarrow \gamma\gamma$ decay by combining EMCal clusters assuming that they are produced by photons originating from the collision vertex. To reduce number of fake π^0 candidates we select clusters with energy $E_\gamma > 0.2 \text{ GeV}$ in $p + p$ and $d + Au$ and $E_\gamma > 0.35 \text{ GeV}$ in $Au + Au$ collisions. Shower profile cut is used to reject broader showers having mostly hadronic origin. In $Au + Au$ collisions we use an asymmetry cut $\alpha = |E_{1\gamma} - E_{2\gamma}| / (E_{1\gamma} + E_{2\gamma}) < 0.8$ to further reduce background since high- p_T combinatorial pairs are peaked at $\alpha = 1$ due to the steeply falling spectrum of single photons. Position and width of the reconstructed π^0 -peak are parameterized as a function of p_T . The width of the π^0 -peak decreases from 12 MeV at $p_T = 1 \text{ GeV}$ to 8 MeV at $p_T > 3 \text{ GeV/c}$. Pairs of photons with invariant mass within two standard deviations of the π^0 -peak position and

transverse momentum $p_T > 1 \text{ GeV}/c$ are selected as π^0 -candidates. The candidates are assigned the exact mass of the π^0 -meson and measured p_T of the pair.

Depending on the decay mode we further combine a π^0 -candidates with other particles in the event. In case of $\omega(\eta) \rightarrow \pi^0\pi^+\pi^-$ decay we combine π^0 candidates with any pair of negatively and positively charged tracks assuming them to be π -mesons. Momenta of the charged tracks are selected to be below $4 \text{ GeV}/c$ and $8 \text{ GeV}/c$ for η and ω respectively. At higher momentum the charged particle spectra are dominated by decay products of long living particles. More details are described in ³. For $\omega \rightarrow \pi^0\gamma$ decay reconstructed π^0 -candidates are combined with all other photons from the same event with energy $E_\gamma > 1 \text{ GeV}$. In case of $K_S^0 \rightarrow \pi^0\pi^0$ decay we combine two π^0 -candidates together. However, if the invariant mass of two most energetic photons assigned to two different π^0 -candidates is within four standard deviations of π^0 -mass then such pair is rejected. This cut suppresses combinatorial background from misidentified π^0 's. To account for K_S^0 -meson life time ($c\tau = 2.7 \text{ cm}$) the decay point for every pair is shifted from the collision vertex by the decay length of K_S^0 along the momentum vector of the pair. Finally we recalculate momenta of the π^0 -candidates and eventually momentum of the pair.

Examples of invariant mass distributions measured in $p + p$ collisions are shown in Figure 1. Mixed event technique does not reproduce background shape for none

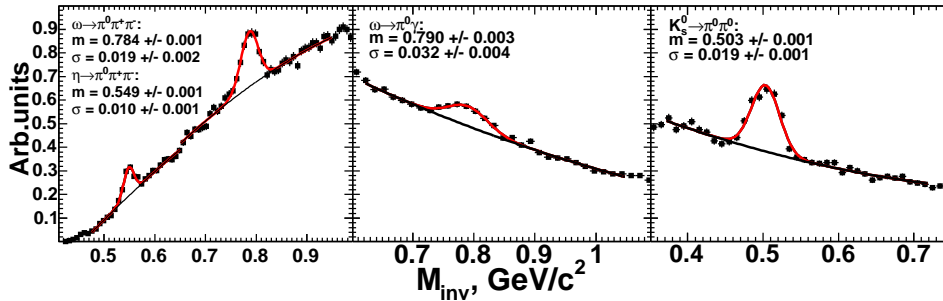


Fig. 1. Invariant mass spectra for different decays at $5 < p_T(\text{GeV}/c) < 6$ in $p + p$ collisions.

of the decays because of particle correlations present in the events. To extract the particle raw yields we use several fitting options. First we fit the peaks with Gaussian function and adjacent background with a parabola as shown in Figure 1. Secondly, the background is approximated in the same region with a parabola, but the points under the peak are rejected from the fit. The parabola interpolated under the peak is subtracted from the histogram. The yield is counted as a sum of the bins in the region initially excluded from the fit. Finally, we narrow the fitting region and use linear function instead of parabolic to describe the background. The three fits are applied to invariant mass spectra collected with different analysis cuts (matching of the charged track to the PC3 hit, tighter cuts for neutral particles) where the

shape of the background distribution is different. The raw yields extracted in each case are fully corrected for reconstruction and trigger efficiencies described further. The first of the described fits with its statistical error is taken as the result and a variance of the six measurements is added to the systematic errors as an estimate of yield extraction uncertainty.

For the evaluation of meson reconstruction efficiencies we use Exodus as a particle generator and PISA (PHENIX Integrated Simulation Application) for full Monte-Carlo simulation of the detector and online trigger settings. For the three body decay of ω and η -mesons the EXODUS is also used as a particle decay engine weighted to reproduce the phase space density^{4,5,6}. The simulation code is tuned to represent the real configuration of the detector subsystems and to make sure that simulated shape, position and width of the π^0 , η , ω and K_S^0 -peaks are consistent with the ones measured in real data at all p_T . Left panel of Figure 2 shows

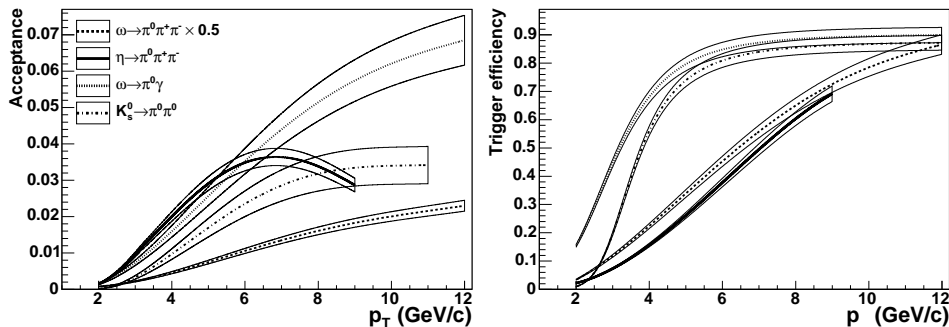


Fig. 2. Geometrical acceptances and meson trigger efficiencies for hadron decays of ω , K_S^0 and η -mesons. Systematic uncertainties are shown with bands.

the acceptance efficiencies which depend on the detector geometry, decay kinematics, performance of detector subsystems and on the cuts used in the analysis. Right panel of Figure 2 shows the high- p_T γ -trigger efficiencies for reconstructed decays in $p+p$. They are recalculated from the measured single photon trigger efficiency using kinematics of the particular decays. Both efficiencies must be taken into account to correct the raw yields measured in high- p_T γ -triggered data samples whereas only the curves shown in the left panel are used in MB samples. In $Au + Au$ events one must account for the additional loss in efficiency caused by cluster overlap in the EMCal. This correction is based on simulated single ω -mesons embedded in real events and reconstructed using the analysis procedure. Percentage of the reconstructed mesons is used to correct for this effect.

Systematic errors for different decay modes of ω and K_S^0 -mesons are summarized in Table 2. Details for η -meson are described in³. Total systematic error of the measurements is dominated by raw yield extraction, meson trigger efficiency and total cross section uncertainties.

Table 2. Relative systematic errors (%) for different decay modes and collision systems. Values with a range indicate variation of the systematic error over the p_T range of the measurement.

Source	$\omega \rightarrow \pi^0 \pi^+ \pi^-$		$\omega \rightarrow \pi^0 \gamma$			$K_S^0 \rightarrow \pi^0 \pi^0$	
	$p + p$	$d + Au$	$p + p$	$d + Au$	$Au + Au$	$p + p$	$d + Au$
Acceptance	5 – 10	9 – 12	10 – 20	8 – 12	14 – 16	10 – 25	10 – 20
Trigger efficiency	3 – 10	5 – 7	2 – 7	5	-	2 – 10	5
Yield extraction	5 – 25	10 – 15	5 – 15	10	15 – 35	7 – 30	9
MB trigger	10	8	10	8	4	10	8
Total	15 – 25	18 – 22	15 – 25	17 – 20	20 – 45	20 – 40	15 – 25

4. Results

The invariant p_T spectra measured for ω -mesons at $\sqrt{s_{NN}} = 200 \text{ GeV}$ are shown in the left panel of Figure 3. In $p + p$ collisions we observe a very good agreement

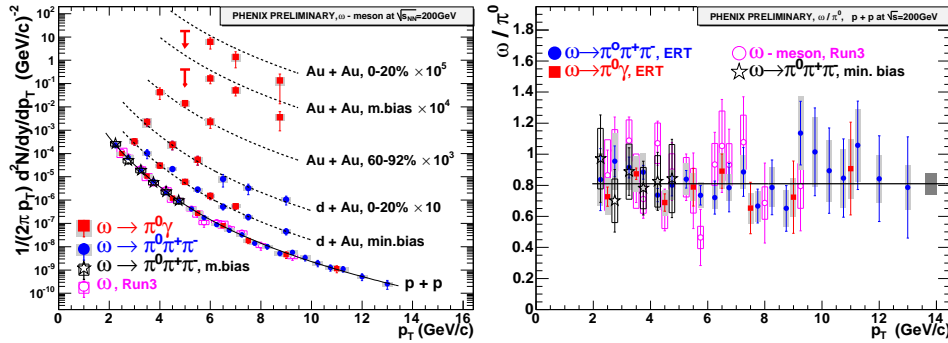


Fig. 3. Left: Invariant p_T spectra for ω -mesons in $p + p$, $d + Au$ and $Au + Au$ collisions at $\sqrt{s_{NN}} = 200 \text{ GeV}$. Right: (ω/π^0) ratio as a function of transverse momentum. Statistical errors are shown with error bars and systematic errors are shown with boxes.

between Run3^{7,8} and Run5 results and between the two decay modes measured in the analysis. In Run5 both the high- p_T and the MB trigger data give consistent results. Dashed curves in $d + Au$ and $Au + Au$ points are the fits to $p + p$ spectrum scaled by the corresponding number of binary collisions. As one can see the production of ω -mesons in $d + Au$ and peripheral $Au + Au$ collisions follows the binary scaling, while in the MB and in the most central $Au + Au$ collisions we observe a suppression of ω -meson production with $R_{AA} = 0.4 \pm 0.15$. Ratio of ω -meson and π^0 -meson spectra² in $p + p$ collisions is shown in the right panel of Figure 3. The ratio is flat in the p_T range of the measurement. Fit to a constant shown with a solid line gives a value of $0.81 \pm 0.02 \pm 0.07$ that agrees with previous PHENIX measurements of $0.85 \pm 0.05 \pm 0.09$ ⁷. Both measurements give a value of the ratio slightly below PYTHIA⁹ prediction of one. Lower energy measurements

of R-806¹⁰ and E706¹¹ collaborations are consistent with the presented results.

In Run3 we also measured $\eta \rightarrow \pi^0\pi^+\pi^-$ decay mode. The result is published in³. From the analysis standpoint this decay is very similar to the ω -meson decay and the result is consistent with the $\eta \rightarrow \gamma\gamma$ measured by PHENIX.

Invariant cross sections of the K -meson production in $p + p$ and $d + Au$ collisions at $\sqrt{s_{NN}} = 200 \text{ GeV}$ are shown in the left panel of Figure 4. The $K_S^0 \rightarrow \pi^0\pi^0$ results are completed with results of charged kaon measurements using PHENIX time-of-flight¹². The p_T range of Run5 measurements extends to $10 \text{ GeV}/c$ providing a baseline for heavy ion measurements. Cross section measured in $p+p$ collisions is consistent with $K_S^0 \rightarrow \pi^+\pi^-$ results from STAR in the overlap region¹³. Dependence of the K/π ratio on transverse momentum is shown in the right panel of Figure 4. Fit to a constant at $p_T > 2 \text{ GeV}/c$ gives a value of $0.45 \pm 0.01 \pm 0.05$.

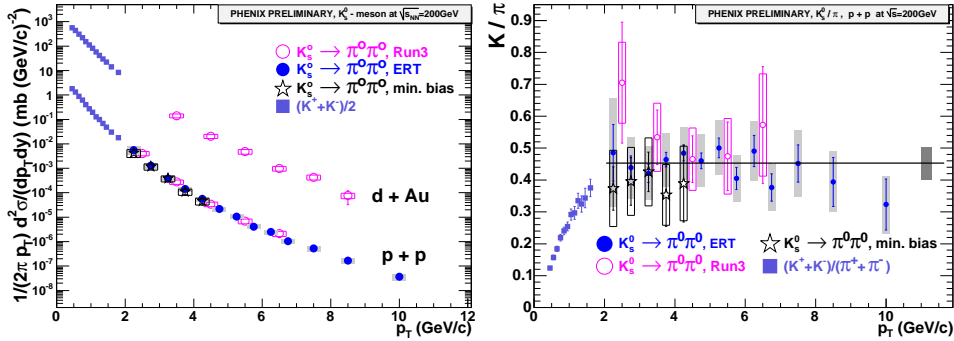


Fig. 4. Left: Invariant cross section for K -mesons in $p+p$ and $d+Au$ collisions at $\sqrt{s_{NN}} = 200 \text{ GeV}$. Right: K/π^0 ratio as a function of transverse momentum. Statistical errors are shown with error bars and systematic errors are shown with boxes.

References

1. K. Adcox *et al.*, *Nucl. Instr. Meth.* **A499** (2003) 469-479.
2. S. S. Adler *et al.*, *Phys. Rev. Lett.* **91** (2003) 241803.
3. S. S. Adler (PHENIX Collaboration), 2006 arXiv: nucl-ex/0611006.
4. S. Giovannella (KLOE Collaboration), 2005 arXiv: hep-ex/0505074.
5. C. Alf *et al.*, *Phys. Rev. Lett.* **9** (1962) 325-327.
6. M. L. Stevenson *et al.*, *Phys. Rev.* **125** (1962) 687-690.
7. S. S. Adler (PHENIX Collaboration), 2006 arXiv: nucl-ex/0611031.
8. Yu. Riabov (PHENIX Collaboration), 2007 arXiv: nucl-ex/0702022.
9. PYTHIA 6.2006, T. Sjostrand *et al.*, hep-ph/0108264 used with default parameters.
10. M. Diakonou *et al.*, *Phys. Lett.* **B89** (1980) 432-436.
11. L. Apanasevich *et al.*, FERMILAB-Pub-00/054-E (2000).
12. S. S. Adler *et al.*, *Phys. Rev.* **C74** (2006) 024904.
13. B. I. Abelev (STAR Collaboration), 2006 arXiv: nucl-ex/0607033.

International Journal of Modern Physics E
© World Scientific Publishing Company

INSTRUCTIONS FOR TYPESETTING MANUSCRIPTS USING COMPUTER SOFTWARE*

FIRST AUTHOR[†]

*University Department, University Name, Address
City, State ZIP/Zone, Country[‡]
first_author@university.edu*

SECOND AUTHOR

*Group, Laboratory, Address
City, State ZIP/Zone, Country
second_author@group.com*

Received (received date)

Revised (revised date)

The abstract should summarize the context, content and conclusions of the paper in less than 200 words. It should not contain any references or displayed equations. Typeset the abstract in 8 pt Times roman with baselineskip of 10 pt, making an indentation of 1.5 pica on the left and right margins.

1. General Appearance

Contributions to *International Journal of Modern Physics E* are to be in English. Authors are encouraged to have their contribution checked for grammar. American spelling should be used. Abbreviations are allowed but should be spelt out in full when first used. Integers ten and below are to be spelt out. Italicize foreign language phrases (e.g. Latin, French).

The text is to be typeset in 10 pt roman, single spaced with baselineskip of 13 pt. Text area (including copyright block) is 8 inches high and 5 inches wide for the first page. Text area (excluding running title) is 7.7 inches high and 5 inches wide for subsequent pages. Final pagination and insertion of running titles will be done by the publisher.

*For the title, try not to use more than 3 lines. Typeset the title in 10 pt Times roman, uppercase and boldface.

[†]Typeset names in 10 pt Times roman, uppercase. Use the footnote to indicate the present or permanent address of the author.

[‡]State completely without abbreviations, the affiliation and mailing address, including country. Typeset in 8 pt Times italic.

2 *Authors' Names*

2. Major Headings

Major headings should be typeset in boldface with the first letter of important words capitalized.

2.1. *Sub-headings*

Sub-headings should be typeset in boldface italic and capitalize the first letter of the first word only. Section number to be in boldface roman.

2.1.1. *Sub-subheadings*

Typeset sub-subheadings in medium face italic and capitalize the first letter of the first word only. Section numbers to be in roman.

2.2. *Numbering and spacing*

Sections, sub-sections and sub-subsections are numbered in Arabic. Use double spacing before all section headings, and single spacing after section headings. Flush left all paragraphs that follow after section headings.

2.3. *Lists of items*

Lists may be laid out with each item marked by a dot:

- item one,
- item two.

Items may also be numbered in lowercase roman numerals:

- (i) item one
- (ii) item two
 - (a) Lists within lists can be numbered with lowercase roman letters,
 - (b) second item.

3. Equations

Displayed equations should be numbered consecutively in each section, with the number set flush right and enclosed in parentheses

$$\mu(n, t) = \sum_{i=1}^{\infty} 1(d_i < t, N(d_i) = n) \int_{\sigma=0}^t 1(N(\sigma) = n) d\sigma. \quad (1)$$

Equations should be referred to in abbreviated form, e.g. “Eq. (1)” or “(2)”. In multiple-line equations, the number should be given on the last line.

Displayed equations are to be centered on the page width. Standard English letters like x are to appear as x (italicized) in the text if they are used as mathematical symbols. Punctuation marks are used at the end of equations as if they appeared directly in the text.

Theorem 1. *Theorems, lemmas, etc. are to be numbered consecutively in the paper. Use double spacing before and after theorems, lemmas, etc.*

Proof. Proofs should end with □

4. Illustrations and Photographs

Figures are to be inserted in the text nearest their first reference. Where possible, figures should be embedded in electronic form from scanned images or a computer-based drawing package. Otherwise, original india ink drawings of glossy prints are preferred. Please send one set of originals with copies. If the author requires the publisher to reduce the figures, ensure that the figures (including letterings and numbers) are large enough to be clearly seen after reduction. If photographs are to be used, only black and white ones are acceptable.

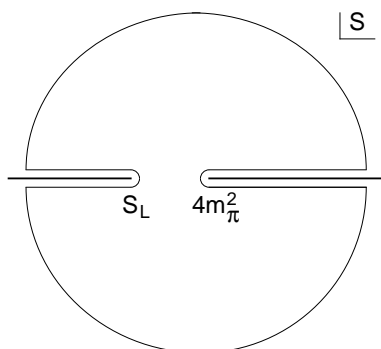


Fig. 1. A schematic illustration of dissociative recombination. The direct mechanism, $4m^2_\pi$ is initiated when the molecular ion S_L captures an electron with kinetic energy.

Figures are to be sequentially numbered in Arabic numerals. The caption must be placed below the figure. Typeset in 8 pt Times roman with baselineskip of 10 pt. Use double spacing between a caption and the text that follows immediately.

Previously published material must be accompanied by written permission from the author and publisher.

5. Tables

Tables should be inserted in the text as close to the point of reference as possible. Some space should be left above and below the table.

4 *Authors' Names*

Table 1. Comparison of acoustic for frequencies for piston-cylinder problem.

Piston mass	Analytical frequency (Rad/s)	TRIA6- S_1 model (Rad/s)	% Error
1.0	281.0	280.81	0.07
0.1	876.0	875.74	0.03
0.01	2441.0	2441.0	0.0
0.001	4130.0	4129.3	0.16

Note: Table notes

^aTable footnote A

^bTable footnote B

Tables should be numbered sequentially in the text in Arabic numerals. Captions are to be centralized above the tables. Typeset tables and captions in 8 pt Times roman with baselineskip of 10 pt.

If tables need to extend over to a second page, the continuation of the table should be preceded by a caption, e.g. “*Table 2. (Continued)*”

6. References

References in the text are to be numbered consecutively in Arabic numerals, in the order of first appearance. They are to be typed in superscripts after punctuation marks, e.g. “. . . in the statement.⁵”

References are to be listed in the order cited in the text. Use the style shown in the following examples. For journal names, use the standard abbreviations. Typeset references in 9 pt Times roman.

7. Footnotes

Footnotes should be numbered sequentially in superscript lowercase roman letters.^a

Acknowledgements

This section should come before the References. Funding information may also be included here.

Appendix A. Appendices

Appendices should be used only when absolutely necessary. They should come after the References. If there is more than one appendix, number them alphabetically. Number displayed equations occurring in the Appendix in this way, e.g. (A.1), (A.2), etc.

^aFootnotes should be typeset in 8 pt Times roman at the bottom of the page.

$$\mu(n, t) = \sum_{i=1}^{\infty} 1(d_i < t, N(d_i) = n) \int_{\sigma=0}^t 1(N(\sigma) = n) d\sigma. \quad (\text{A.1})$$

References

1. J. Callaway, *Phys. Rev.* **B35** (1987) 8723.
2. M. Tinkham, *Group Theory and Quantum Mechanics* (McGraw-Hill, New York, 1964).
3. T. Tel, in *Experimental Study and Characterization of Chaos*, ed. B. Hao (World Scientific, Singapore, 1990), p. 149.
4. P. P. Edwards, in *Superconductivity and Applications — Proc. Taiwan Int. Symp. on Superconductivity*, ed. P. T. Wu *et al.* (World Scientific, Singapore, 1989), p. 29.
5. W. J. Johnson, Ph.D. Thesis, Univ. of Wisconsin, Madison, 1968.
6. P. F. Marteau and H. D. I. Arbabanel, “Noise reduction in chaotic time series using scaled probabilistic methods”, UCSD/INLS preprint, October 1990.